Metrohm Autolab

Application Area: Corrosion

Electrochemical Corrosion Studies of Various Metals

Keywords

Metrohm Autolab, Autolab Microcell HC, corrosion, 1.4301 stainless steel, thin film, nickel, S235 steel, polarization resistance technique, electrochemical impedance spectroscopy, potentiodynamic polarization technique, Tafel extrapolation.

Introduction

Corrosion is the degradation of a material over time, caused by environmental effects [1]. Corrosion of metals is a problem seriously affecting not only many industrial sectors, but also private life, resulting in enormous costs. According to government and industry studies, over 220 billions of dollars are lost to corrosion in the United States each year [2]. Therefore, protection against corrosion is a large research field and many different approaches exist, depending on the desired application and environmental requirements.

Common corrosion protection methods are, for example, the application of paint on metals, preventing direct contact between the metal and the corrosive medium; the usage of inhibitors, which scavenge the corrosive substances in the medium; or the cathodic protection, where a potential difference forces the corrosion to occur on a sacrificial anode.

Various types of corrosion exist, being classified based on morphology or mechanism. Subdivisions are uniform, crevice, pitting or localized corrosion; environmentally assisted or stress corrosion; cracking and galvanic corrosion. Galvanic corrosion, typically resulting in a rather rapid attack, occurs if a less noble metal is in (electrical) contact with a nobler metal in an electrolyte.

External electrical currents, like stray ground currents from large electrical equipment, could be an additional source of potential differences, resulting in galvanic corrosion.

Due to the numerous types of corrosion occurring on different materials in various environments, numerous publications dealing with a specified problem using a test method adapted to the distinct environmental requirements exist [2-4]. As a consequence, the results are hardly comparable and only few general measurement norms are available [5]. In this application note, the results gained during electrochemical corrosion studies on different metals are compared to literature data. Unfortunately, in literature corrosion rates for the different metals using the same testing method could not be found. Therefore, the experiments presented here will change depending on different specimens, in order to reproduce the test methods reported in literature at best.

Besides, the exact metal composition of the sample under investigation and other details like surface treatment during fabrication, are not exactly described, even if they influences the corrosion rate [6]. In corrosion science, the question about the duration of some corrosion event is of extreme importance, like how long a particular corrosion process will last, before resulting in a leak or in a vessel rupture. Thus, knowing the corrosion rates is of high interest. Unfortunately, corrosion rates are also know to vary. This leads, in some cases, to an unpredictable quantification. Nevertheless, if their limitations are understood, corrosion rates can be really useful and, therefore, they have been published for numerous combinations of materials and environments. Typically, these rates are averages over many tests, as the result of a single sample may deviate distinctly from the mean [2]. Usually, corrosion rates are given as mass loss per unit area and per unit time or by means of the thickness loss as rate of penetration, and expressed either as milli inches per year, mpy or millimeter per year mmpy [4].

The damage caused by corrosion is evaluated either by studying mass or thickness losses with time, or by electrochemical methods [4]. While the first method often requires larger test specimen and longer times, the second one is more suitable for laboratory use. Corrosion rates of less than 3 mpy are acceptable for most chemical processes and structures. Materials showing rates between 2 and 20 (partially 50) mpy are considered useful for the given environment, while those exhibiting higher rates are usually unacceptable [1].

Short summary of corrosion theory

The oxidation of a metal exposed to a strong acid is one of the most basic corrosion reactions. For example, pure iron in hydrochloric acid results in the gradual disappearance of the iron specimen and the formation of hydrogen bubbles [1]:

$$Fe(s) + 2HCl(aq) \rightarrow Fe^{2+}(aq) + 2Cl^{-}(aq) + H_2(g) \quad (1)$$

Thereby, an iron atom is oxidized to an iron ion Fe^{2+}, by releasing two electrons, which are taken by the hydrogen ions

coming from the dissolution of hydrochloric acid. The hydrogen ions are thus reduced and form hydrogen gas. The electron transfer occurs at the iron surface [1]. The faster the dissolution of the metal, the higher the current flow. The overall corrosion reaction can be divided in the cathode and anode half-cell reaction, here with their respective standard redox potentials [1]:

$$\begin{array}{ll} 2H^+(aq) + 2e^- \rightarrow H_2(g) & 0.0\ V \\ Fe(s) \rightarrow Fe^{2+}(aq) + 2e^- & +0.44\ V \end{array} \qquad 2$$

The standard redox potential of the respective reactions is tabulated and deviations from the standard conditions can be calculated using the Nernst equation [1, 7].

$$E = E_0 - \frac{RT}{nF}\ln\frac{[red]}{[ox]} \qquad 3$$

Where E is the electrode potential, E_0 the standard cell potential, R is the gas constant (8.314 J/(mol·K)); T is the temperature in Kelvin; n is the number of transferred electrons; F is the Faraday constant (96485 C/mol) and [red] and [ox] are the concentrations of the reduced and oxidized species, respectively.

The larger the difference between potentials of the anodic and cathodic half-cell reaction, the higher the driving force for the reaction. In a closed electrochemical circuit, current begins to flow and the potentials of both half-cell reactions move towards each other. The resulting net current is the sum of the current coming from the oxidation reaction, called anodic or oxidation current, and the current opposite in sign coming from the reduction reaction, called cathodic or reduction current. The point at which the anodic and the cathodic currents are equal defines the corrosion potential E_{corr}. The magnitude of the current is the so-called corrosion, current i_{corr}. The corrosion current cannot be measured directly, since it is exactly balanced by the cathodic current, which at E_{corr} has the same magnitude but opposite in sign. However, it is possible to estimate i_{corr} with a variety of techniques discussed later in the text.

Butler-Volmer formalism for a half-cell reaction

In the case of a current flowing through an electrochemical cell, the half-cell potentials shift from their equilibrium values with the deviation called overpotential or overvoltage η [7]:

$$\eta = E(i) - E \qquad 4$$

Where E is the half-cell equilibrium potential, given by the Nernst equation (Equation 3) and E(i) is the potential represented as function of current density i [7].

In electrochemical systems where the reaction rate is determined by the charge transfer at the metal surface, like for corrosion measurements in the vicinity of E_{corr}, the current-to-voltage relation is described by the Butler-Volmer equation [7, 8]:

$$i = i_a + i_c = \\ = i_0\left\{exp\left[\frac{\alpha nF}{RT}\eta\right] - exp\left[-\frac{(1-\alpha)nF}{RT}\eta\right]\right\} \qquad 5$$

Where i, is the current density of the complete reaction, i_a and i_c are the current densities of the anodic and cathodic branches, respectively, i_0 is the exchange current density, α is the transfer coefficient, which describes the charge transfer kinetics and ranges between 0 and 1. The other parameters have the same meaning as described in Equation 1 [8]. When |η| is distinctly larger than RT/nF = 25.7 mV at 25 °C, the respective counter-reaction can be neglected. This is usually the case when |η| is higher than 50 mV. For the cathodic branch this results into:

$$i = -i_0 exp\left[-\frac{(1-\alpha)nF}{RT}\eta\right] \qquad 6$$

After taking the logarithm and rearranging Equation 6, η can be expressed as:

$$\eta = -\frac{RT}{(1-\alpha)nF}2.3\log i_0 - \frac{RT}{(1-\alpha)nF}2.3\log|i| \qquad 7$$

Thus yielding the form of a linear equation $\eta = A + B\cdot\ln|i|$. This type of notation is known as Tafel form [8]. Please note that log is the logarithm to the basis 10, and 2.3 is the conversion factor between $\log_e$ and $\log_{10}$.

The same holds for the anodic branch:

$$i = i_0 exp\left[-\frac{\alpha nF}{RT}\eta\right] \\ \eta = -\frac{RT}{\alpha nF}2.3\log i_0 + \frac{RT}{\alpha nF}2.3\log|i| \qquad 8$$

A constant B, called Tafel constant, can be defined for both the anodic (B_a) and cathodic (B_c) branches, as:

$$B_a = \frac{2.3RT}{\alpha nF} \qquad B_c = \frac{2.3RT}{(1-\alpha)nF} \qquad 9$$

Corrosion analysis

As discussed above, if the two half-cell reactions are in equilibrium a mixed potential E_{corr} is reached. Deviations from equilibrium are induced by applying an external positive or negative polarization potential E_{ext} to the system. Small deviations are associated with the charge transfer polarization overpotential η_{CT}:

$$\eta_{CT} = E_{ext} - E_{corr} \qquad 10$$

During corrosion analysis it is assumed that, over the potential range of interest, the contribution of the currents of the respective reverse reactions (in this case, the reduction of iron and the oxidation of hydrogen), are negligible [7]. Thus, the equations for the oxidation and reduction current densities i_{ox} and i_{red}, respectively, reduce to:

$$i_{ox} = i_{corr} exp\left[\frac{2.3}{B_{a,M}}\eta_{CT}\right]$$
$$|i_{red}| = i_{corr} exp\left[-\frac{2.3}{B_{c,X}}\eta_{CT}\right] \qquad 11$$

By definition, the cathodic current density is set as negative. Thus, for the resulting current density holds: $i = i_a + i_c = i_a - |i_c|$, [7, 9].

Thereby, $B_{a,M}$ and $B_{c,X}$ symbol the Tafel constants of the metal oxidation branch and the reduction branch of the species to be reduced respectively. Please note that in corrosion science the exchange current density close to E_{corr} is labeled corrosion current density i_{corr}; this convention will be complied in the subsequent manuscript. The measured current density i_{meas} is the difference of the oxidation and reduction current density:

$$i_{meas} = i_{ox} - |i_{red}| =$$
$$= i_{corr}\left\{exp\left[\frac{2.3}{B_{a,M}}\eta_{CT}\right] - exp\left[-\frac{2.3}{B_{c,X}}\eta_{CT}\right]\right\} \qquad 12$$

As can be seen from this equation, if η_{CT} approaches zero, $|i_{meas}|$ also approaches zero as the current resulting from the oxidation reaction equals that of the reduction reaction.

Thus, the net flow is zero and the curves become asymptotic to the corrosion potential, E_{corr}, see Figure 1 where $|i_{meas}|$ is plotted in logarithmic scale as function of η_{CT}.

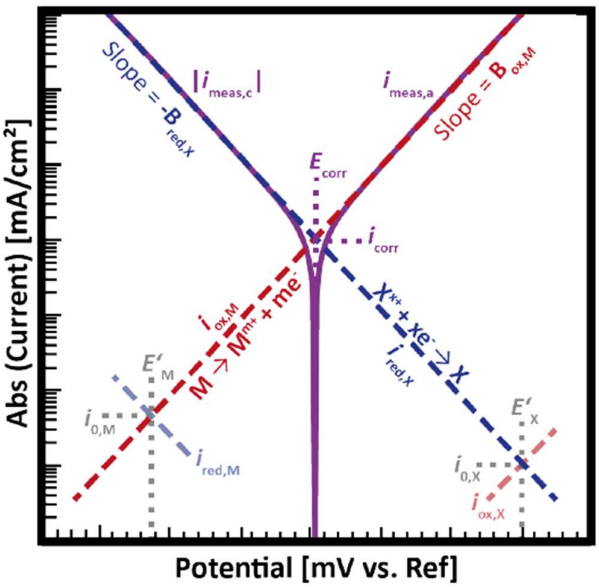

Figure 1 - Schematic experimental polarization curves (violet) plotting the logarithm of the absolute value of the measured current density assuming Tafel behavior for the individual oxidation (red) and reduction (blue) reaction polarization curves. Slopes of the individual linear regions correspond to the respective Tafel constant. M, M^{m+}, X^{x+} and X symbol the oxidized and reduced form of metal and the species being reduced during corrosion experiments (e.g. hydrogen), respectively, E'_M and E'_X the respective equilibrium half-cell potential, $i_{0,M}$ and $i_{0,X}$ the respective exchange current density, $i_{red,M}$ and $i_{red,X}$, $I_{ox,M}$ and $I_{ox,X}$ the respective reduction and oxidation current density of the two half-cell reactions (given for the example above in Equation 2). Modified and redrawn from [7].

At this point, a state of dynamic equilibrium exists and i_{ox} as well as i_{red} are equal to the exchange current density and thus the corrosion current density. It can be determined by extrapolation of the respective Tafel equation to the linear portion of the cathodic and anodic branch of the measured current: At sufficient large positive or negative overpotentials (Equation 11) reduces to the equation of a single oxidation or reduction reaction, respectively, as the respective other exponential becomes negligible and the branches become linear, thus corresponding to the respective Tafel equation. This equation would plot exactly like the respective linear portion in Equation 12, but it would extend as shown by the dashed portion of the line in Figure 1. The intersection of both extrapolations delivers the corrosion potential as well as the corrosion current. If only one branch shows sufficient linear portion – in most cases the cathodic branch - the intersection

of the dashed extension with the ordinate value corresponding to E_{corr} is the corrosion current. For many metals and alloys the anodic branch does not show sufficient linear portion due to active-passive behavior. In case the corrosion is under diffusion control or the nature of the interface changes with changing potential a linear region may be also not observed in the cathodic branch [7].

in case of small overvoltages of less than 10 mV, and assuming equal values for both the transfer coefficient of the metal oxidation $\alpha_{a,m}$ and that of the reduction of the species to be reduced $\alpha_{c,X}$, i.e. $\alpha = \alpha_{a,m} = \alpha_{c,X}$, the exponents are small enough that the series expansion of Equation 11 can be truncated after the second term ($e^x = 1 + x$ for small x) resulting in the following expression for the Butler-Volmer equation [8]:

$$i = i_{corr}\left\{1 + \frac{\alpha nF}{RT}\eta_{CT} - \left[1 - (1-\alpha)\frac{nF}{RT}\eta_{CT}\right]\right\} = \\ = i_{corr}\frac{\alpha nF}{RT}\eta_{CT} \qquad 13$$

Thus, for $|\eta_{CT}| < 10$ mV the current-overpotential curves become linear with a slope only dependent on i_{corr} but not on α [8]. The term $RT/nFi_{corr} = d\eta/di$, i.e. the slope of the line, has units of resistance, thus being labeled polarization resistance R_p, which can also be expressed using the Tafel constants B_a and B_c:

$$\frac{d\eta}{di} = \frac{B_{a,M} \cdot B_{c,X}}{2.3 \cdot i_{corr} \cdot \left(B_{a,M} + B_{c,X}\right)} = R_p \qquad 14$$

This equation is derived from Equation 13 by insertion the expressions for Tafel constants B_a and B_c:

$$i = i_{corr}\left\{1 + \frac{2.3}{B_{a,M}}\eta_{CT} - \left[1 - \frac{2.3}{B_{C,X}}\eta_{CT}\right]\right\} = \\ = 2.3 i_0 \frac{B_{a,M} + B_{c,X}}{B_{a,M} \cdot B_{c,X}}\eta_{CT} \qquad 15$$

Solving this expression for i_{corr} leads to

$$i_{corr} = \frac{B_{a,M} \cdot B_{c,X}}{2.3R_p\left(B_{a,M} + B_{c,X}\right)} \qquad 16$$

Which is often used in corrosion science in case the Tafel slopes are known for the reaction under investigation for calculation of the i_{corr} from the corrosion resistance.

R_p can be used for determination of i_{corr} [2]. Please note, that this is only a rough assumption as for real samples the α values could differ from each other significantly. In this case, values for the Tafel constants either determined from experiments or taken from literature have to be used for calculation of i_{corr}, see Equation 16. After determination of the corrosion current density the corrosion rate can be calculated using Faraday's law with n as number of transferred electrons, W as weight of the electroactive species, i.e. the mass of the species that has reacted, F as Faraday constant, M as atomic weight and t as time [7]:

$$i_{corr} = \frac{nWF}{Mt} \qquad 17$$

M/n is the so-called equivalent weight, defined as the atomic weight of the element divided by the valence of the element, i.e., the number of electrons required to oxidize an atom of the element in the corrosion process [5].

Solving Equation 17 for W/t and dividing it by the density ρ of the material results in the corrosion penetration rate CPR, in cm/s:

$$CPR = \frac{Mi_{corr}}{nF\rho} \qquad 18$$

More commonly, CPR is expressed as mmpy (mm per year) or mpy (milli inches per year) [7]:

$$CPR(mmpy) = C_{mmpy}\frac{Mi_{corr}}{nF\rho} \\ CPR(mpy) = C_{mpy}\frac{Mi_{corr}}{nF\rho} \qquad 19$$

With $C_{mmpy} = 3.27 \cdot 10^{-3}$ mm·mol/(µA·cm·y) and $C_{mpy} = 0.129$ mi·mol/(µA·cm·y), respectively, with y the year; mi the milli inch. The corrosion current i_{corr} is given in units of µA/cm^2, otherwise the constants need to be adapted.

Electrochemical methods for corrosion studies

There are several electrochemical methods for studying corrosion phenomena and determining the corrosion rates [2, 7]. In the following section, four well established procedures will be shortly presented.

Polarization resistance technique

A very well established method for both corrosion prediction and monitoring is the linear polarization or polarization

resistance technique [2]. It is not only a rapid, simple, and relatively inexpensive technique, but it can be also applied without detailed knowledge of the controlling electrochemical parameters in complex, poorly defined electrolytes [2]. Using this method, the realistic limit for corrosion rate estimation is about 0.001 mm/year (0.1 mpy) mostly because of limitations in estimating Tafel slopes [2]. The ASTM standard G59 describes the general test procedure. In this method, the specimen is stored for 55 minutes in the test solution for determination of the (open circuit) corrosion potential E_{corr} [7]. Thereafter, a potentiodynamic polarization curve is recorded starting 30 mV more negative and ending 30 mV more positive than E_{corr} [5]. The polarization resistance is the reciprocal of the slope of the polarization curve at the corrosion potential, when the current is plotted versus the voltage. As long as the polarization is in the vicinity of the corrosion potential, i.e., approx. ± 30 mV or less, the measurement does not interfere with the quantities being measured [2]. In consequence, as the material surface is expected to remain unchanged, repeated measurements can be performed without preparing the sample before each measurement [7]. For calculation of the corrosion current, see the definition of R_P, Equation 14 and Equation 16 for i_{corr}. The two Tafel constants, i.e. the slopes of the anodic and cathodic branch of the measured curve, and the polarization resistance, all measured at the corrosion potential, are required. Their determination usually requires regression analysis [2].

Electrochemical impedance spectroscopy

Electrochemical impedance spectroscopy is also a routine tool for practical corrosion prediction [2]. It enables a rapid estimation of corrosion rates lower than 0.0001 mm/year and can be applied even in low-conductivity media [2]. Using a suitable equivalent circuit the corrosion resistance can be determined. Using the definition of R_P or Equation 16, it can be used for calculation of the corrosion current density. Thus, partly knowledge of the Tafel constants for the given material system might be required [7]. If they are unavailable or not easily obtained, a value of 25 mV can be used for Tafel constant $B = (B_a \cdot B_c)/[2.3(B_a + B_c)]$, likewise assuming equal values for both transfer coefficients $\alpha_{a,M}$ and $\alpha_{c,X}$ [2, 5]. However, this might result in errors greater than 50% [2].

Potentiodynamic polarization technique

Like the linear polarization resistance method the (cyclic or anodic) potentiodynamic polarization technique continuously ramps the applied potential usually starting at the corrosion potential in direction of more positive potential [2]. Partially, the voltage is reversed at some chosen potential and scanned in cathodic or active direction to the corrosion potential or a potential active with respect to it [2]. ASTM standard G61 describes the general test procedure. This technique is used for prediction of localized corrosion, but should not be used to determine the uniform rate of corrosion as the latter case would require the assumption that the corrosion mechanism does not change over a potential range of several hundred millivolts which may not be valid [2]. Potentiodynamic polarization curves are interpreted using the relationship between current and voltage as well as differences between forward and reverse scan thus delivering information about, for example, the repassivation or protection potential, and the pitting potential [2]. However, since the main focus of this application note is the determination of corrosion rates, details about these features and their determination from measurement data are beyond the scope of this report. A detailed discussion about such features, as well as limitations and pitfalls of all electrochemical techniques presented here can be found in literature [2].

Tafel extrapolation

Another technique for determination of uniform corrosion rates is the Tafel extrapolation [7]. In this technique, the applied potential is likewise continuously ramped, but over a medium potential range of usually ± 300 mV vs. E_{corr} [7]. Such a broad potential range (greater than ± 50 to 100 mV compared to E_{corr}) is required to reach potentials at which either the anodic or cathodic reaction dominates (i.e., 25.7/n mV to guarantee for reaching the linear region and some range to actually perform the linear extrapolation) [7]. However, as result of such large deviations from E_{corr}, conditions at the metal/solution interface may change progressively, including iR drops between working and reference electrode or diffusion of species from and to the interface, and prevent linear behavior [7]. For reliable Tafel extrapolation, the current is required to be linear at least over one decade [7].

In general, during corrosion analysis, assuming linearity for determination of Tafel slopes where the curve is actually nonlinear has been estimated to cause errors as high as 50% [2]. However, this may be acceptable as corrosion rates estimated from mass loss can result in errors of 100% [2]. In consequence, during screening, rates differing by a factor of 2 or 3 may be considered to be the same [2].

Experimental

For electrochemical determination of the corrosion rate of the different metal specimens, a TSC surface cell in combination with an Autolab Microcell HC setup has been used, Figure 2.

This cell enables the electrochemical characterization of solid/liquid interfaces and surface characterization of planar, moisture-, air-, or photosensitive substrates of variable shape under temperature control. The PEEK casing guarantees air-tight sealing of the cell. The O-ring pressed from above onto the surface of the sample restricts the active area to 0.283 cm^2.

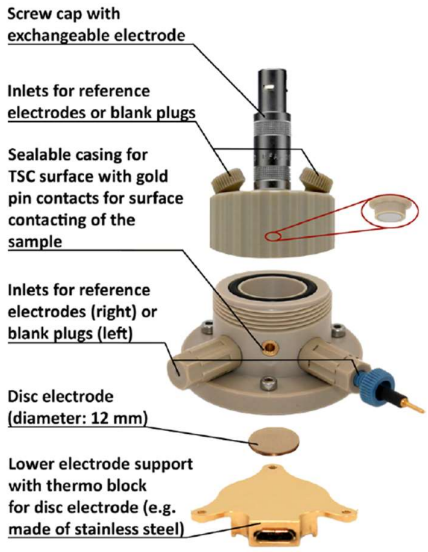

Figure 2 - Exploded view of measuring cell TSC surface.

The solid sample is placed on the lower electrode. Its active surface is restricted by an O-ring being pressed from above onto it. For surface studies of the solid sample the gold pin contacts are used for contacting. The liquid electrolyte is inserted from above. The two plugs laterally screwed into the casing enable the insertion of reference electrodes. The inlets in the cap also enable the employment of reference electrodes or can be used as gas inlet/outlet.

Besides, a Metrohm Autolab PGSTAT204 equipped with a FRA32M module was used for the electrochemical analysis. For data acquisition, the NOVA software has been employed. In the Autolab Microcell HC setup, temperature is controlled via a Peltier element which enables temperatures from -40 °C up to +100 °C, depending on dew point and sample amount. In combination with a Microcell HC setup, the temperature accuracy is 0.1 °C in the thermo block. The composition of the different metallic specimen is given in Nickel thin films (TF) were electrochemically deposited onto polished stainless steel substrates.

Table 1 - Composition and fabrication details of the metal specimen characterized in this application note.

Alloy	Composition (%)	Fabrication remarks
Stainless steel 1.4301	C ≤ 0.07 P ≤ 0.05 Mn ≤ 2.00 Si ≤ 1.00 Cr 17.5 - 19.5 S ≤ 0.03 Ni 8.00 - 10.5 N ≤ 0.11 Fe Balance	(a) turned of stainless steel rod (b) laser cut from rolled stainless steel sheet, polished down to grain size of 1 µm (c) laser cut from rolled stainless steel sheet, abrasive paper of grid size 1200
Nickel thin film	pure nickel	Electrochemical deposition at 40 °C on polished stainless steel; either 3 min at 3 V or 6 min at 2 V
Steel S235	C ≤ 0.22 Cr ≤ 0.3 Mn ≤ 1.6 Si ≤ 0.05 P ≤ 0.05 S ≤ 0.05 Cu ≤ 0.3 N ≤ 0.012 Fe Balance	-

In the case of stainless steel 1.4301, three differently treated sets of specimen were studied to investigate the influence of the surface treatment on the corrosion rate. While one set of specimen was taken from a stainless steel rod (a), the other two sets were laser-cut from a rolled stainless steel sheet. One set was polished using diamond paste down to a grain size of 1 µm (b) and the other one was treated using abrasive paper grid size 1200 with ethylene glycol (c).

Experimental procedures for the different metal specimen were adopted from the respective literature and are summarized in Table 2. Only the potential windows were reduced, since at potentials far away from E_{corr}, the formation of gas bubbles (presumably H_2) occurs, leading to partial contact loss. However, the potential windows have been selected wide enough for proper Tafel evaluation. Finally, the pH of the electrolyte used for corrosion study of the nickel thin films was adjusted using dilute sulfuric acid.

Table 2 - Experimental procedure for the different metal specimen together with the respective literature specified in the square brackets. Potentials were recorded vs. Ag/AgCl (3 mol/l KCl) reference.

Alloy Literature	Electrolyte	Potential range (V)	Scan Rate (mV/s)	T (°C)
Stainless steel 1.4301 [10]	2 mol/l HCl	- 0.45 to - 0.17*	1.66	20.0
Nickel thin film [11]	0.5 mol/l Na_2SO_4 (pH ~ 2)	- 0.55 to + 0.15	1.00	25.0
Steel S235 [12]	0.5 mol/l HCl	- 0.70 to - 0.40	0.50	25.0

* For one single measurement of the polished specimen the upper potential limit was set to -0.25 V, linear Tafel analysis was nevertheless possible.

In each case, the respective specimen and a 6 mm diameter polished platinum electrode were used as working and counter electrode, respectively. As reference electrode, a Ag/AgCl electrode (+210 mV/NHE, checked vs. commercial Ag/AgCl reference) was used made of a silver wire coated with AgCl in 3 mol/l KCl solution and in contact with the cell compartment via a ceramic frit. Approximately 0.9 ml of the respective electrolyte were inserted into the measuring cell.

Electrochemical studies were performed at the respective temperatures given in Table 2. Normally, measurements were started directly after the assembling of the cell and after a short determination of the open circuit potential. Before the polarization experiment (depending on the corrosive behavior of the sample-electrolyte combination) an impedance spectrum was recorded at open circuit potential in a 3-electrode configuration for frequencies from 500 kHz down to 10 Hz, with an amplitude of 10 mV (rms). If the sample-electrolyte combination was too corrosive so that corrosion along with bubble formation took already place during impedance measurement, the latter measurement was skipped. Linearity was proofed for the frequency range of interest using Kramers-Kronig Test [7, 14].

Results and discussion

For each different metal specimen, at least three measurements were performed as common in literature [12, 13]. For Tafel evaluation, the measured current density was plotted on logarithmic scale vs. the applied potential and slopes of the cathodic and anodic branch were determined via linear extrapolation of the respective linear region of the curve. Corrosion rates were calculated using equivalent weights tabulated in ASTM standard G102. The resulting mean values for the corrosion rate, the corrosion current as well as the corrosion potential are summarized in Table 3 together with the values reported in literature.

Table 3 – Mean values for the corrosion rate, the corrosion current density as well as the corrosion potential for the different metal specimen. Errors are given as maximal deviation from the mean. The respective literature values are given in brackets. Potentials were recorded vs. Ag/AgCl (3 mol/l KCl) reference. Different treatment of the stainless steel (SS) specimen: (a) turned of stainless steel rod; (b) laser cut from rolled stainless steel sheet, polished; (c) laser cut from rolled stainless steel sheet, abrasive paper.

Alloy	E_{corr} (V)	Error E_{corr} (%)	i_{corr} ($\mu A/cm^2$)	Error i_{corr} (%)	CPR (mmpy)	Error CPR (%)
SS (a)	- 0.382	4.9	297.02	14.6	3.050	14.6
(b)	- 0.325	3.5	6.963	5.8	0.072	5.8
(c)	- 0.330	11.4	6.374	17.1	0.065	17.1
[10]	(- 0.365)		(400)		(4.3)	
Nickel thin film [11]	- 0.127 (- 0.121)	20.3	1.695 (0.55)	34.9	0.018 (0.006)	34.9
Steel S235 [12]	- 0.546 (- 0.607)	0.5	253.1 261.9	8.6	2.97 (3.07)	8.6

Examples of polarization curves for each of the diverse metal specimen are presented in Figure 3 to Figure 5.

Stainless steel 1.4301

Comparison of the corrosion potential determined for the rod-shaped stainless steel samples with the one reported in literature reveals a good agreement with only minor difference of 0.017 V. The corrosion rate calculated for the studies presented in this application note is approximately 30% lower than the literature value, thus also showing sufficient agreement taking into account the diverging results normally expected in corrosion studies, so that corrosion rates diverging by a factor of two to three are regarded as equal [2].

Regarding the differently pretreated stainless steel 1.4301 specimen laser-cut from a rolled stainless steel sheet, there is only a negligible difference in corrosion potential of 0.005 V between polished and by abrasive paper treated ones. For the latter samples the corrosion current and thus the rate was less than 10% lower than for the polished one, thus also showing good agreement. With respect to the diverging results normally expected in corrosion studies, the difference observed for the two different surface treatments should be within this error and thus insignificant [2].

In contrast, the set of rod-shaped stainless steel samples showed corrosion rate more than 42 times higher in comparison to the samples taken from rolled metal sheets and the corrosion potential is shifted to more negative potentials. In literature, both beneficial and detrimental effects of rolling are reported [8, 15, 16]. Positive effects of cold rolling resulting in reduced corrosion rates are caused by, for example, hardening, tailoring the microstructures or by a higher Cr:Fe ratio in the passive surface film [15 - 17].

The shift of the corrosion potential to more noble potentials as well as a reduced corrosion current density for rolled stainless steel specimen in comparison to untreated ones was reported by Phandis et al. comparing rolled and annealed 1.4301 stainless steel in 3.5% NaCl solution [17]. Annealing of stainless steel specimen after rolling is expected to revoke the positive effect of rolling [16].

Warzee et al. also emphasized the great impact of initial surface treatment of stainless steel on the corrosion rate and revealed cold-work, i.e. rolling, polishing or grinding, as essential factor for lowering of the corrosion rate, while definition of the surface state in terms of its roughness is inadequate [6]. However, in the study of Warzee et al., the beneficial effect of cold-work was only observed in superheated steam at temperatures higher than 350 °C, but not at lower temperatures or in water. Due to the rather different conditions between Warzee et al. study and the ones applied in this application note, a direct comparison of the results is rather questionable and they only can be seen as hint reinforcing our results of (a) the lower corrosion rate of the rolled stainless steel specimen in comparison to the untreated ones and (b) the corrosion rate being independent of the different surface roughness achieved by either polishing or usage of abrasive paper.

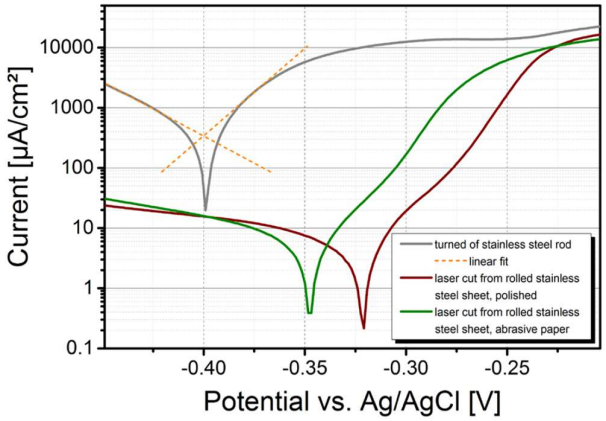

Figure 3 - Representative plot of the polarization curves of the three differently treated stainless steel 1.4301 specimen used for determination of E_{corr} and i_{corr} by Tafel analysis. For sake of clarity, the linear fits are only shown for the rod-shaped stainless steel specimen, but they were performed for all other samples analyzed using Tafel analysis. The scan speed and the temperature during measurement were 1.66 mV/s and 20.0 °C, respectively. The stainless steel specimen were used as working electrode, while platinum and 2 mol/l HCl were employed as counter electrode and electrolyte, respectively.

Nickel thin films

The results reported in Table 3 for the nickel thin films are the mean values of thin films deposited at 3 V and 2 V, resulting in current densities during thin film preparation of approximately 0.32 A/cm^2 and 0.07 A/cm^2, respectively. For each different fabrication, two specimen were examined. In accordance with literature, the corrosion potential of the thin films deposited at higher current density is slightly lower than for the ones prepared at lower one. However, the mean difference of E_{corr} is only 0.011 V, thus natural fluctuation during corrosion studies also could not excluded as basic cause. More detailed investigations with specimen prepared at more than two different current densities would be required for a more reliable statement, which is beyond the scope of this application note. The range of E_{corr} reported in literature for the nickel thin films deposited using diverse current densities ranging from 0.01 to 0.10 mA/cm^2 is from -0.121 to -0.213 V. The value determined during the experiments presented in this application note fits with -0.127 V in this range. However, as in the literature source the corrosion potential decreases with increasing deposition current density, a lower value would be expected during our studies. Nevertheless, as not only the deposition current density, but also the total film thickness might influence the corrosion behavior, a more detailed comparison is not possible based on the published data and beyond the scope of this application note.

Corrosion current and thus the corrosion rate determined during measurements for this application note are approximately three times the mean of the values reported in literature. However, taking into account the different deposition conditions during thin film preparation together with the natural fluctuation of corrosion rates, the accordance is still sufficient [2].

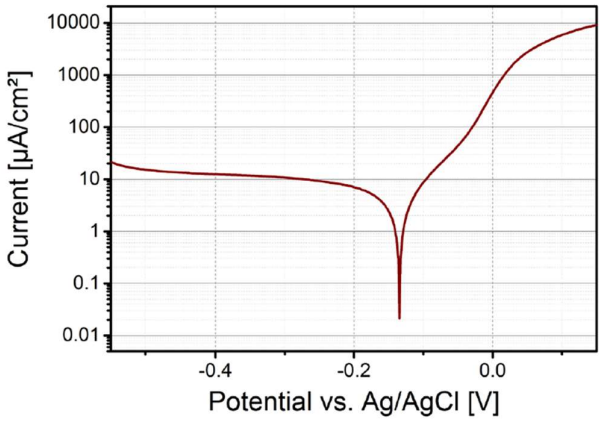

Figure 4 – Representative plot of the polarization curve of nickel thin films used for determination of E_{corr} and i_{corr} by Tafel analysis. Scan speed and temperature during measurement were 1.00 mV/s and 25.0 °C, respectively. The nickel thin film was used as working electrode, while platinum and 0.5 mol/l Na_2SO_4 (pH ~ 2) were employed as counter electrode and electrolyte, respectively.

Steel S235

E_{corr} determined for the S235 steel specimen during measurements is approximately 0.06 V higher than reported in literature. However, as only one literature source could be found, its reliability could not be proved and a difference of only 0.06 mV nevertheless shows good accordance. Comparison of the corrosion rates shows very good agreement, which also should hold for the corrosion current. However, in literature a value half of that calculated from our data is reported, which obviously does not fit to the reported corrosion rate. Inspection of the plots used for Tafel analysis in the literature source also point to higher corrosion currents. It thus stands to reason that erroneous i_{corr} were presented in the literature source, while for calculation of the corrosion rate correct ones were used. Thus, in Table 3 the corrected value recalculated from the corrosion rate given in the literature source is represented.

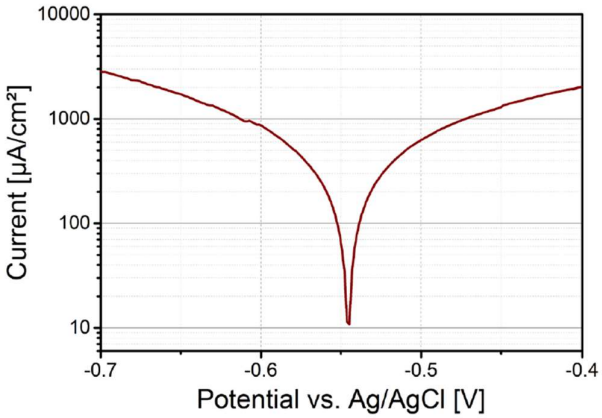

Figure 5 - Representative plot of the polarization curve of steel S235 used for determination of E_{corr} and i_{corr} by Tafel analysis. Scan speed and temperature during measurement were 0.50 mV/s and 25.0 °C, respectively. The steel specimen were used as working electrode, while platinum and 0.5 mol/l HCl were employed as counter electrode and electrolyte, respectively.

Comparison between results achieved using different corrosion test methods exemplarily shown at nickel thin film specimen.

Impedance spectroscopy

In Figure 6, an example of an impedance spectrum recorded for a nickel thin film sample is shown. The equivalent circuit also presented in this figure was used for fitting of the data. Thereby, L symbols an inductor and represents the parasitic inductive artefacts at high frequencies due to e.g. connection cables. R_b is an ohmic resistor and typifies the resistance of the cables as well as the resistance due to bulk ion transport. R_p is the polarization resistance. The constant phase element CPE takes interface effects, such as the charging of the electrochemical double layer at the electrode/sample electrode/electrolyte interface, into account.

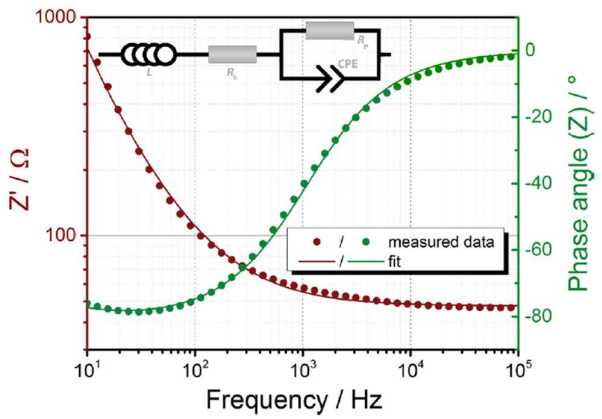

Figure 6 – Bode plot of the impedance measurement of a nickel thin film sample plotting on the left and right ordinate the real part of the impedance Z' and the phase angle, respectively, together with the equivalent circuit representing the impedance behavior of the samples within the chosen frequency range.

Polarization resistance technique

For the determination of the polarization resistance R_p via polarization resistance technique, the data recorded for the Tafel extrapolation were also used, although in this evaluation technique only a small potential range around E_{corr} is measured. For the determination of R_p, the measured current density was plotted linearly vs. the applied potential, see Figure 7, and the slope of the data in the vicinity of the corrosion potential was determined using linear regression, thus delivering the reciprocal of R_p. the corrosion current i_{corr} was calculated either from Equation 13, solved for i_{corr}:

$$i_{corr} = \frac{RT}{nF} \cdot \frac{di}{d\eta_{CT}} = \frac{RT}{nFR_p} \qquad 20$$

Or Equation 16. Examples of results are presented for the nickel thin films in Table 4, comparing the corrosion current density and corrosion rate as well as the respective errors determined using Tafel extrapolation, impedance spectroscopy and polarization resistance technique. For the latter two techniques, results calculated either using Equation 20, i.e. calculation based on universal constants without usage of Tafel slopes, or Equation 16, employing the Tafel slopes, were given.

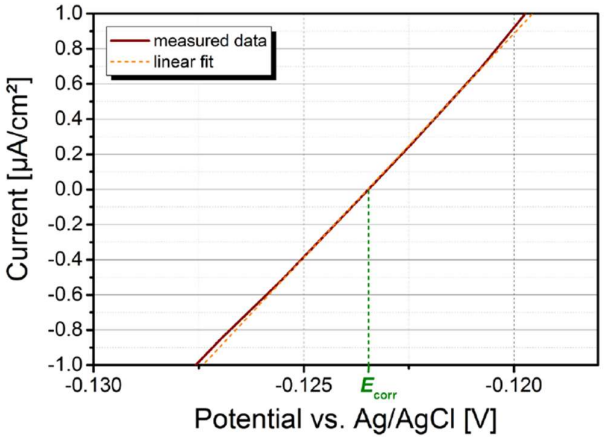

Figure 7 - Representative plot of the polarization curve of nickel thin films showing the linear range close to E_{corr} used for determination of icorr by polarization resistance technique together with the linear fit displayed as dashed line. The scan speed and the temperature during measurement were 1.00 mV/s and 25.0 °C, respectively. The nickel thin film was used as working electrode, while platinum and 0.5 mol/l Na_2SO_4 (pH ~ 2) were employed as counter electrode and electrolyte, respectively.

Values of the corrosion current density and thus of the corrosion rate determined using polarization resistance technique are slightly higher than by application of Tafel extrapolation. This finding was also reported in literature [9, 18]. In contrast, those determined using impedance spectroscopy are slightly lower. However, the agreement between all three techniques is acceptable.

Calculation of i_{corr} using either Equation 16 or Equation 20, i.e., with or without usage of Tafel slopes, respectively, delivers comparable values for both the polarization resistance technique and impedance spectroscopy. For both techniques, the usage of Tafel slopes results in slightly higher values and errors. This thus indicates that Tafel slopes are, at least for the nickel thin film electrodes, not needed for calculation of the i_{corr}, but reliable values can also be achieved using Equation 20, employing universal constants. However, care has to be taken by usage of Equation 20 as during its derivation the assumption was made that both transfer coefficients $\alpha_{a,M}$ and $\alpha_{c,X}$ are equal. This seems to be suitable for the nickel thin film electrodes presented in this application note as usage of Equation 20 delivers values of i_{corr} comparable to the other two techniques applied. However, in case of systems with unknown transfer coefficients, the calculation of i_{corr} should not be solely based on Equation 20, as diverging transfer coefficients for metal oxidation and/or reduction of the species to be reduced could result in distinct errors.

Table 4 - Comparison of the corrosion current density and corrosion rate as well as the respective errors determined using different electrochemical analysis methods for the nickel thin films. Errors are given as maximal deviation from the mean. Method (a) uses Equation 20 for calculation, i.e. calculation based on universal constants without usage of Tafel slopes, while (b) uses Equation 16 employing the Tafel slopes determined during Tafel extrapolation.

Analysis method	i_{corr} ($\mu A/cm^2$)	Error i_{corr} (%)	CPR (mmpy)	Error CPR (%)
Tafel extrapolation	1.695	34.9	1.66	34.9
Polarization resistance technique				
(a)	2.647	23.6	0.029	23.6
(b)	3.13	30.6	0.034	30.6
Impedance spectroscopy				
(a)	0.987	13.6	0.011	13.6
(b)	1.180	44.9	0.013	44.9

The good agreement of all three different techniques used for the determination of i_{corr} leads to the conclusion that at least for the metal specimen investigated in this study, Tafel extrapolation is not needed. Such technique is accompanied by longer measurements and sample preparation after every measurement, due to surface changes during potential scan. Therefore, faster techniques like polarization resistance technique or impedance spectroscopy also deliver reliable results.

Bibliography

[1] Corrosion Engineering Handbook, P.A. Schweitzer (Ed.), 1996, Marcel Dekker, Inc.

[2] Uhling's Corrosion Handbook, 3rd Edition, R. Winston Revie (Ed.), 2011, John Wiley & Sons, Inc.

[3] M. Pourbaix, Biomaterials 5, 3 (1984), 122-134

[4] A. Cinitha et al., KSCE Journal of Civil Engineering 18, 6 (2014), 1735-1744

[5] e.g. ASTM standards G5, G59, G61, G102

[6] M. Warzee et al., J. Electrochem. Soc. 112, 7 (1965), 670-674

[7] Fundamentals of Electrochemical Corrosion, E. E. Stansbury, R. A. Buchanan, 2000, ASM International

[8] Elektrochemie, C. H. Hamann, W. Vielstich, 3. Völlig überarbeitete und erweiterte Auflage 1998, Wiley-VCH

[9] Lehrbuch der Physikalischen Chemie, G. Wedler, Fünfte vollständig überarbeitete und aktualisierte Auflage 2004, Wiley-VCH

[10] R. T. Loto et al., J. Mater. Environ. Sci. 6, 9 (2015) 2409 2417

[11] D. E. Rusu et al., J. Coat. Technol. Res. 9, 1 (2012) 87-95

[12] D. Gassama et al., Bull. Chem. Soc. Ethiop. 29, 2 (2015) 299-310

[13] C. Kuphasuk et al., J. Prosthetic Dentistry 85, 2 (2001), 195-202

[14] J. M. Esteban, M. E. Orazem, J. Electrochem. Soc. 138, 1, (1991), 67-76

[15] L. Peguet et al., Corrosion Science 49 (2007) 1933–1948

[16] C. Garcìa et al., Corrosion Science 43 (2001) 1519–1539

[17] S.V. Phadnis et al., Corrosion Science 45 (2003) 2467–2483

[18] R. Mishra et al., Corrosion Science 46 (2004) 3019–3026

Remarks

Data and report presented in this application note were taken from application note "Electrochemical corrosion studies of various materials" by RHD Instruments GmbH & Co. KG.

Date

September 2019 AN-COR-010

For more information

Additional information about this application note and the associated NOVA software procedure is available from your local **Metrohm distributor**. Additional instrument specification information can be found at **www.metrohm.com/en/products/electrochemistry**.